frontiers | Frontiers in Environmental Science

TYPE Original Research
PUBLISHED 26 January 2023
DOI 10.3389/fenvs.2023.1105408

OPEN ACCESS

EDITED BY
Liming Wang,
Xi'an Polytechnic University, China

REVIEWED BY
Youlian Zhou,
Geology Institute of China Chemical Geology and Mine Bureau, China
Tianguo Li,
Yunnan Agricultural University, China

*CORRESPONDENCE
Li Jiang,
jl@jsut.edu.cn

SPECIALTY SECTION
This article was submitted to Toxicology, Pollution and the Environment, a section of the journal Frontiers in Environmental Science

RECEIVED 22 November 2022
ACCEPTED 12 January 2023
PUBLISHED 26 January 2023

CITATION
He X, Chen X, Wang X and Jiang L (2023), Optimization of activated carbon production from corn cob using response surface methodology.
Front. Environ. Sci. 11:1105408.
doi: 10.3389/fenvs.2023.1105408

Optimization of activated carbon production from corn cob using response surface methodology

Xiaoxue He, Xuexue Chen, Xinran Wang and Li Jiang*

School of Resources and Environmental Engineering, Jiangsu University of Technology, Changzhou, China

Waste management and valorization of waste is a major global issue. Low-cost and renewable adsorbent activated carbon (AC) from agriculture residues is a focus of worldwide concern. Microwave heating is an efficient technology for production of AC. CCAC was synthesized from corn cob *via* microwave vacuum pyrolysis under ambient vacuum, and the optimization process for maximized CCAC yield and its iodine number was developed using response surface methodology (RSM). These regression models have high Fisher test value and lower *p*-value, which ensure its reliability and applicability. The optimized parameters obtained are 550.62 W, 9.26 min, -0.05 Mpa, and 1.7 IR with responses of 37.57% yield and 933.38 mg/g iodine number. The predicted results were validated, and it was found that the experimental data varied only by 4.21% in yield and 4.02% in iodine number from the predicted values. The prepared adsorbent was characterized using instrumental techniques like FT-IR, BET, and SEM. The pyrolysis approach produced CCAC containing regular and homogeneous porous structure with a specific surface area of up to 995.05 m^2/g and total volume of 0.708 cm^3/g.

KEYWORDS

corn cob, activated carbon, response surface methodology, optimization, microwave

1 Introduction

In recent years, solid waste management has been ranked alongside water and air pollution as the most intricate environmental issue in China. According to the Paris Agreement, the Chinese government announced that it has targeted achieving carbon neutrality before 2060. Significant attention has recently been focused on agricultural waste and its role in the transition of societies around the world to circular economies (Fu et al., 2022; Yang et al., 2022).

As one of the world's largest agricultural countries, China produces vast amounts of agricultural waste each year. Agricultural wastes are lignocellulosic materials that can be used as precursors in many conversion techniques, such as pyrolysis, to produce various products, viz., feedstock, biofuels, valuable chemical products, and energy. Although recent research has focused on the use of Chinese waste as soil amendments, AC, and fuels, the majority of them are burned on-site, and the disposal of agricultural wastes from combustion can have adverse effects on people and the environment (Ji et al., 2022).

Corn is one of China's most important cereal crops. In 2020, corn accounted for almost 25% of the total cereal crops in China (NBSC, 2021). Corn cobs (CC) are essential inedible residues after corn production, comprising large amounts of corn residues in China each year, inevitably followed by the generation of large amounts of agricultural waste corn cob due to the approximate 18 kg of corn cob per 100 kg of corn grain production (Tsai et al., 2001). Corn cob is a rich biomass resource, and many studies have been conducted for its various applications (Menardo et al., 2015; Takada et al., 2018; Czajkowski et al., 2019; Ji et al., 2022). Most agricultural residues can be treated as feed or compost, but corn cob cannot be used owing

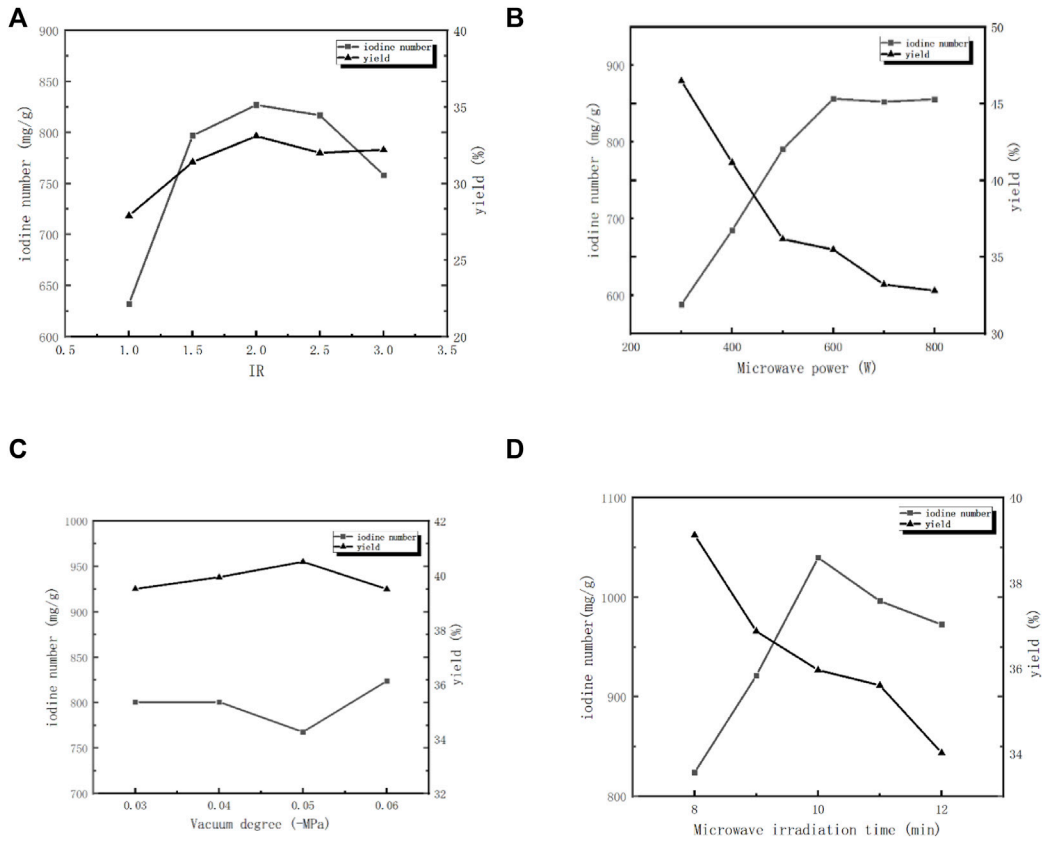

FIGURE 1
Effects of operating factors on the yield and iodine number of AC **(A)** IR, **(B)** microwave power, **(C)** vacuum degree, and **(D)** microwave irradiation time.

to its lack of nutrients. However, corn cob serves as a potential raw material that is locally available and practically used in the experiment, given its rich carbon content and wide abundance, where AC can be derived *via* pyrolysis (Aditya and Zi, 2022).

Agricultural wastes can be converted to AC by conventional and microwave pyrolysis (Scarlett et al., 2022). The main difference between microwave and conventional pyrolysis is the heating method; the microwave method involves volumetric heating, while conventional pyrolysis involves conduction or convection heating (Shukla et al., 2019; Selvam and Paramasivan, 2022). Conventional pyrolysis is achieved using a bath furnace with high thermal inertia and low electricity conversion efficiency (Arpia et al., 2021). Microwave-assisted pyrolysis has a higher efficiency in the heating process because energy transfer is facilitated through the interaction of molecules inside the biomass rather than heat transfer from external sources (Zi et al., 2019; Li et al., 2022). The main advantages of microwave heating are shorter retention time, better overall efficiency, and a faster and more controllable process (Elsa and James, 2017; Arpia et al., 2021; Yu et al., 2022). Several studies have reported the product optimization of diverse biomass using microwave pyrolysis, e.g., lignin (Tayra and Maraísa, 2022), horse manure (Mong et al., 2020), oil palm (Idris et al., 2022), corn cob (Quillope et al., 2021), sugarcane bagasse (Selvam and Paramasivan, 2022), and empty fruit bunch (Mohamad, 2022).

Microwave heating technology under vacuum is usually applied in the food processing industry. Microwave vacuum pyrolysis (MVP) represents a promising and innovative pyrolysis approach that has recently been proposed as an alternative to converting biomass into products. Performing pyrolysis under a vacuum environment causes the vacuum environment to replace the need of carrier gas (e.g., nitrogen gas) that is generally used in conventional pyrolysis. Some reports were recently published on microwave vacuum pyrolysis for waste conversion and recovery (Nam et al., 2018; Wan et al., 2018; Yek and Liew, 2019; Shin and Syazana, 2020; Wan and Wai, 2020) involving the application of a vacuum environment to lower the production cost since the need to constantly use inert gas (e.g., nitrogen) during pyrolysis is eliminated and has advantages by avoiding undesirable recondensation reaction and combustion (Liew et al., 2018). The preparation of AC by MVP deserves more attention from researchers, and the optimization of process production could also produce immeasurable environmental and economic benefits (Wan and Wai, 2020).

To the best of our knowledge, the optimal response of the operating factors on iodine number and yield of CCAC and its properties derived through MVP have not yet been reported. The objective of this study is to produce AC from an agricultural waste (corn cob) through microwave heating under ambient vacuum. The RSM-based Central Composite Design (CCD) model was utilized to establish the relative effects of process variables and their interactions, which would assist researchers in exploring opportunities for implementing MVP technology for AC production, thereby producing better-quality AC for sustainable environmental applications.

10.3389/fenvs.2023.1105408

TABLE 1 Coded and actual levels for independent factors used in the experimental design.

Factors	Code	Units	Coded variable levels				
			-α	-1	0	+1	+α
IR	A	-	1	1.5	2	2.5	3
Microwave power	B	W	300	400	500	600	700
Vacuum degree	C	-MPa	0.03	0.04	0.05	0.06	0.07
Microwave irradiation time	D	min	8	9	10	11	12

2 Materials and methods

2.1 Preparation of AC

The corn cob used in this study was obtained from a village in Xuzhou, Jiangsu Province, China. CC was initially washed twice with pure water to remove dust and subsequently dried at 105°C for 24 h to remove moisture. Then, the dried CC was ground and sieved through a 50-mesh sieve. The CC particles were then impregnated with a specific concentration of H_3PO_4 for 12 h.

The impregnation ratio (IR) was estimated from following equation:

$$IR = \frac{weight\ of\ H_3PO_4}{weight\ of\ corn\ cob}. \quad (1)$$

After the reaction was finished, the CC particles were dried for 24 h at 110°C. The dried masses were kept in a microwave oven to produce CCAC. The microwave vacuum pyrolysis of CCAC was performed at different IR, microwave power, microwave irradiation times, and vacuum degrees. After heating, the system was cooled to room temperature, and the obtained samples were washed with 1 M HCl and distilled water until the pH value of the washed solution was between 6 and 7 and then oven-dried at 120°C.

2.2 Experimental design

Statistical experimental design, as an efficient way to improve experimental works, has been widely used in chemistry, food, and environmental engineering (Ji et al., 2022; Kong and Zhi, 2022). Among these design methods, RSM is considered a powerful technique for testing multiple process variables and identifying interactions between these variables, and a combination of factors generating an optimal response can be identified by this technique (Kai et al., 2022). In addition to raw materials, external parameters of activation temperature, activation time, and impregnation ratio play key roles in AC preparation. Accordingly, to determine optimal preparation conditions, the RSM experiment was carried out, and the iodine number (Y1) and yield (Y2) were analyzed as response values. Based on previous single-factor test results, IR, microwave power, vacuum degree, and microwave irradiation time were set in the range of 1–3, 300–700 W, -0.003 MPa to -0.007 MPa, and 8–12 min, respectively.

RSM was employed to optimize the operating conditions of the AC manufacturing process. 1) IR; 2) microwave power; 3) vacuum degree; and 4) microwave irradiation time were optimized by central composite design (CCD). Response Y values were the iodine number (Y1) and yield (Y2) of AC.

2.3 Measurement of iodine number and yield of AC

Iodine number is a widely used parameter to determine the adsorption capacity for simple and rapid assessment of AC quality. The iodine number indicates the porosity of AC, and it is defined as the amount of iodine adsorbed by 1 g of carbon at the milligram level. The iodine adsorption was determined using GB12496.8–2015 (the testing standard for activated carbon in China) (International Continence Society, 2015).

The yield of AC was estimated from following equation:

TABLE 2 Experimental design matrix and results.

Run no	A	B	C	D	Iodine number, Y1 (mg/g)	Yield, Y2 (%)
	IR (-)	Microwave power (W)	Vacuum degree (-MPa)	Microwave irradiation time (min)		
1	2	500	0.07	10	675.55	31.47
2	1.5	400	0.06	9	723.95	34.12
3	1.5	600	0.06	11	832.27	37.9
4	2	500	0.05	10	907.62	36.9
5	2.5	400	0.06	11	730.48	32.47
6	1.5	600	0.04	11	739.38	34.39
7	2.5	400	0.04	11	816.2	35.6
8	2	500	0.05	10	1039.63	35.96
9	2.5	600	0.06	11	619.99	28.91
10	2	500	0.05	10	787.62	36.2
11	2.5	600	0.04	11	580.05	26.99
12	2	500	0.05	10	1016.22	39.84
13	2	500	0.03	10	676.81	32.02
14	3	500	0.05	10	1015.7	39.86
15	2	500	0.05	10	653.3	29.93
16	2	500	0.05	12	1011.22	39.12
17	2	700	0.05	10	800.77	36.51
18	2	300	0.05	10	558.46	32.2
19	1.5	600	0.04	9	1028.86	40.77
20	2.5	600	0.04	9	799.49	34.02
21	1.5	400	0.04	11	852.52	38.22
22	2.5	600	0.06	9	764.23	36.49
23	2	500	0.05	10	807.13	37.43
24	1.5	400	0.06	11	560.02	25.62
25	1.5	400	0.04	9	796.84	35.4
26	2.5	400	0.04	9	769.14	35.85
27	2	500	0.07	10	945.48	38.86
28	1.5	400	0.06	9	792.3	36.14
29	1.5	600	0.06	11	792.5	37.28
30	2	500	0.05	10	559.41	28.12

$$Yield\ of\ AC\ (wt\%) = \frac{weight\ of\ activaed\ carbon}{weight\ of\ corn\ cob}. \quad (2)$$

2.4 Characterization of CCAC

The characteristics of CCAC were determined by nitrogen adsorption at 77 K using a Micromeritics ASAP 2010C surface area analyzer (USA). BET surface area was calculated from N_2 adsorption isotherms by using the BET equation based on the assumption that the area of the nitrogen molecule was 0.162 nm^2. The total pore volume (Vp) was estimated from the volume of N_2 (as liquid) held at a relative pressure (P/P0) of 0.95. The pore size distribution (PSD) of the prepared AC was calculated from adsorption isotherms using the BJH method. The morphology of AC was examined by scanning electron microscopy (Hitachi Co., model S-3400NII). Furthermore, the FT-IR spectra of the raw material and sample were recorded using a Nicolet Nexus 470 FTIR aerator in the range 400–4000 cm^{-1} using KBr pellets at room temperature (Liew et al., 2018).

TABLE 3 Analysis of variance (ANOVA) for iodine number of CCAC.

Source	Sum of squares	df	Mean square	F value	*p*-value Prob > F	
Model	5.652E+005	14	40367.97	15.54	<0.0001	Significant
A	1.493 E+005	1	1.49 E+005	57.46	<0.0001	
B	14920.11	1	14920.11	5.74	0.03	
C	4254.41	1	4254.41	1.64	0.2201	
D	167.69	1	167.69	0.06	0.8029	
AB	44.62	1	44.62	0.02	0.8975	
AC	6292.46	1	6292.46	2.42	0.1405	
AD	24.26	1	24.26	0.01	0.9243	
BC	4332.27	1	4332.27	1.67	0.2162	
BD	1094.29	1	1094.29	0.42	0.5262	
CD	5081.55	1	5081.55	1.96	0.1823	
A^2	1.967 × 105	1	1.97 × 105	75.72	<0.0001	
B^2	87362.67	1	87362.67	33.62	<0.0001	
C^2	1.236 × 105	1	1.24 × 105	47.57	<0.0001	
D^2	1.272 × 105	1	1.27 × 105	48.96	<0.0001	
Residual	38972.94	15	2598.2			

TABLE 4 Analysis of variance (ANOVA) for yield of CCAC.

Source	Sum of squares	df	Mean square	F value	*p*-value Prob > F	
Model	354.57	14	25.33	3.82	0.0072	Significant
A	159.29	1	159.29	24.01	<0.0001	
B	8.53	1	8.53	1.29	0.2746	
C	1.62	1	1.62	0.24	0.6287	
D	1.54	1	1.54	0.23	0.6374	
AB	1.57	1	1.57	0.24	0.6338	
AC	27.22	1	27.22	4.1	0.061	
AD	0.02	1	0.02	0.01	0.9581	
BC	4.07	1	4.07	0.61	0.4457	
BD	0.2	1	0.2	0.03	0.8659	
CD	2.26	1	2.26	0.34	0.5683	
A^2	51.9	1	51.9	7.82	0.0135	
B^2	17.52	1	17.52	2.64	0.0125	
C^2	63	1	63	9.5	0.0076	
D^2	72.03	1	72.03	10.86	0.0049	
Residual	99.52	15	6.63			

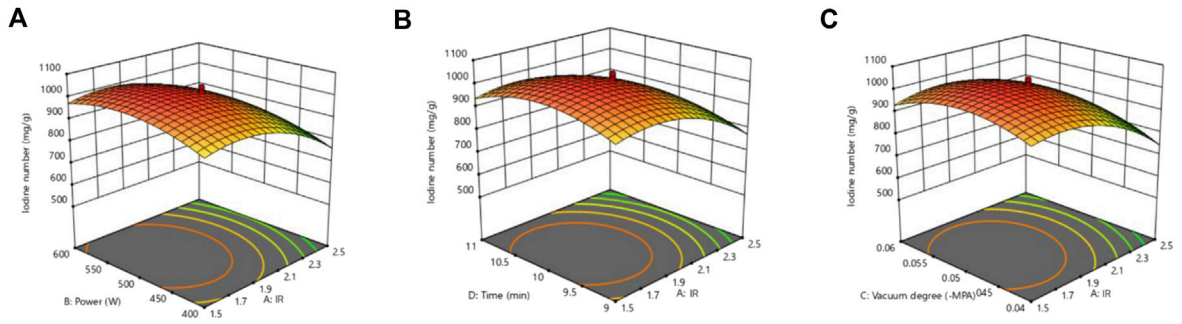

FIGURE 2
Combined effects of **(A)** IR and power, **(B)** IR and time, and **(C)** IR and vacuum degree on iodine number of CCAC.

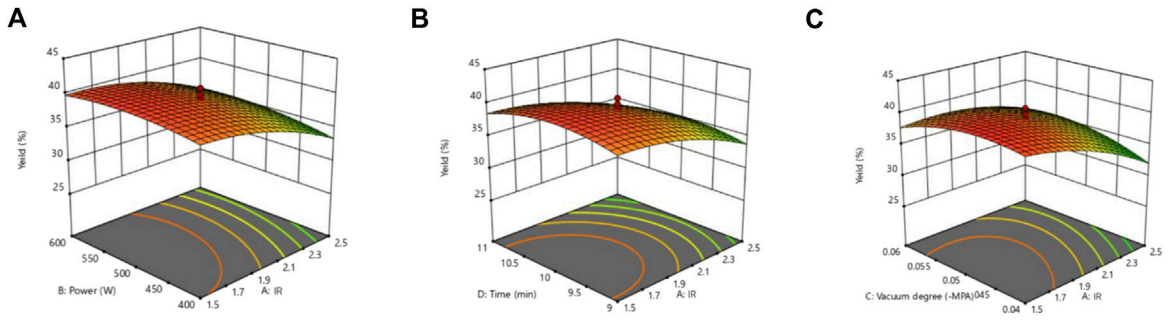

FIGURE 3
Combined effects of **(A)** IR and power, **(B)** IR and time, and **(C)** IR and vacuum degree on yield of CCAC.

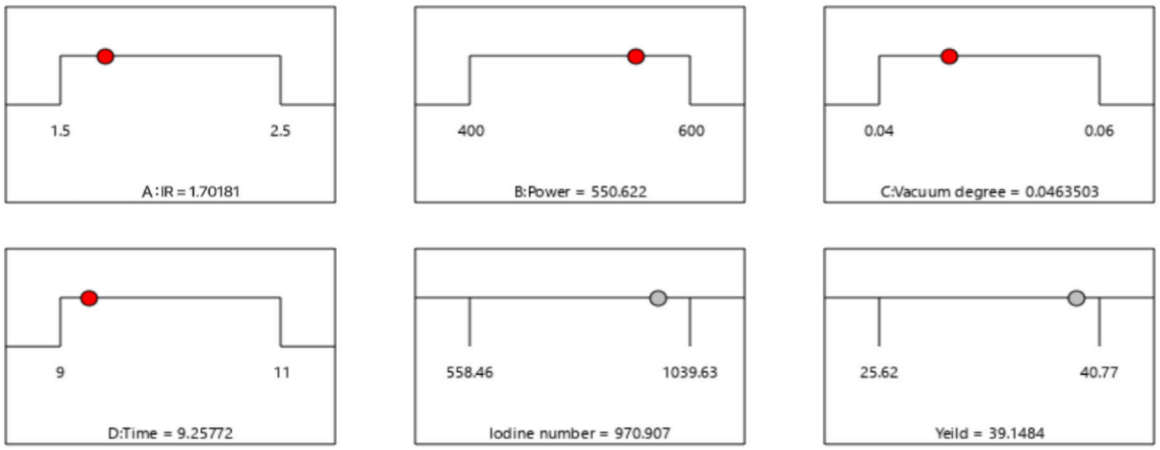

FIGURE 4
Optimized process slope shape.

TABLE 5 Comparison of predicted and experimental results on iodine number and yield.

Operating conditions	Iodine number (mg/g)			Yield (%)		
A = 1.7, B = 550.62 W, C = -0.05 MPa, and D = 9.26 min	Experimental	Predicted	Error (%)	Experimental	Predicted	Error (%)
	933.38	970.91	4.02	37.57	39.15	4.21

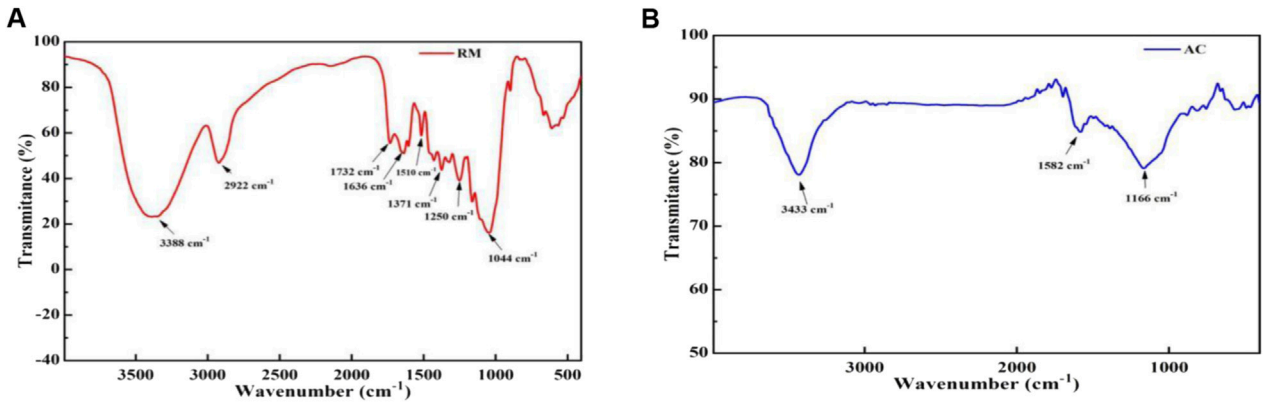

FIGURE 5
(A) Infrared spectrum of CC; **(B)** infrared spectrum of CCAC.

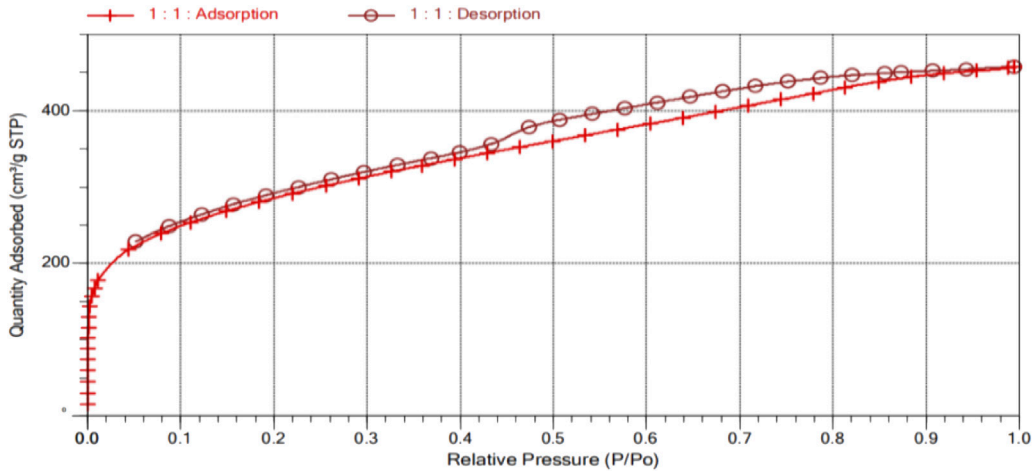

FIGURE 6
N^2 adsorption–desorption isotherm of CCAC.

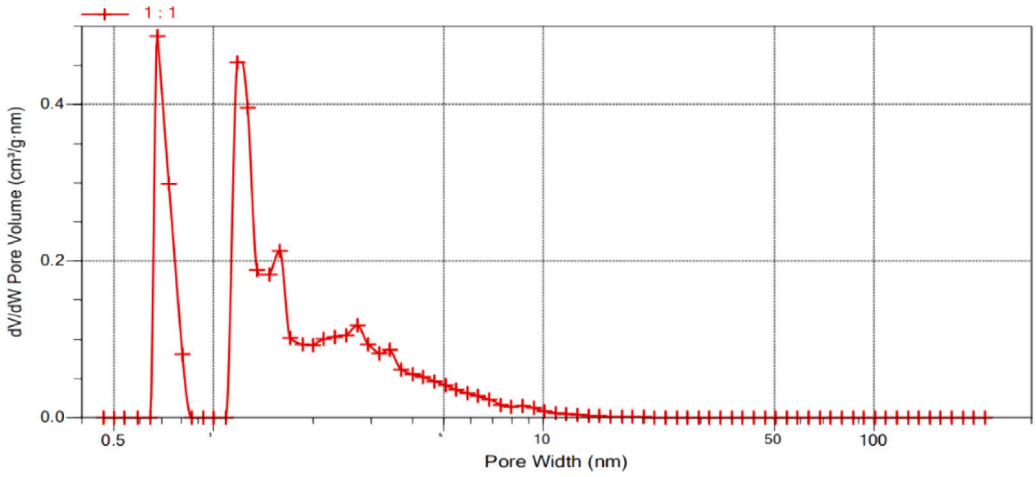

FIGURE 7
Pore size distribution of CCAC.

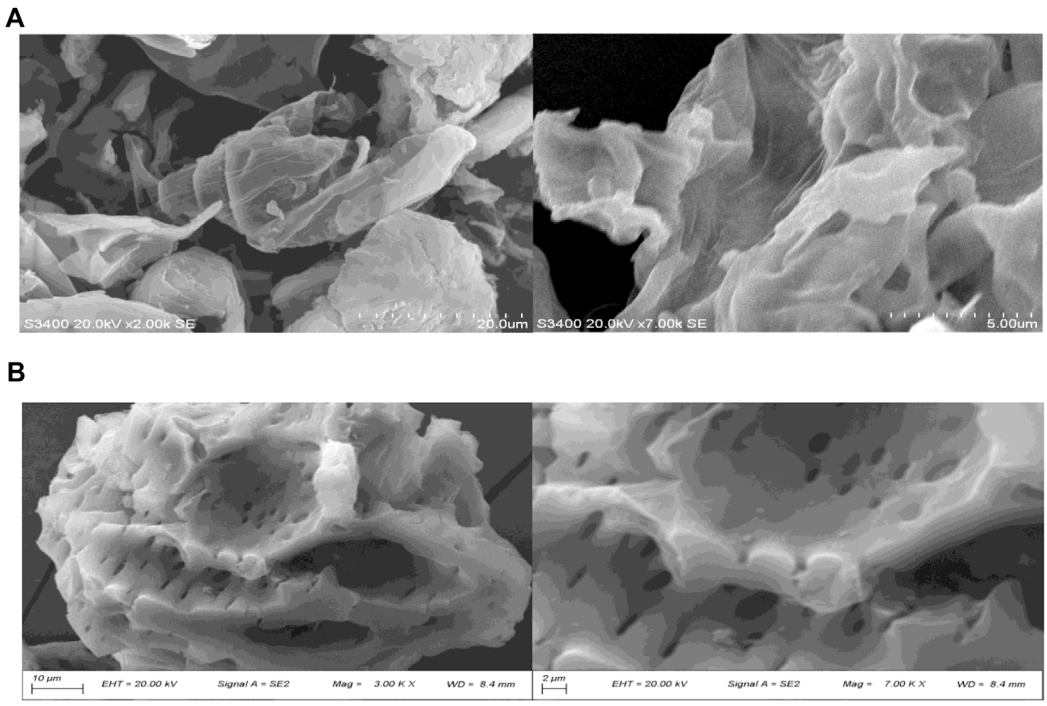

FIGURE 8
(A) SEM photographs of raw material; **(B)** SEM photographs of CCAC.

3 Results and discussion

3.1 Single-factor experiments

3.1.1 Impregnation ratio

The impregnation ratio is crucial to development of the pores of the adsorbent material. As shown in Figure 1A, with the change in impregnation ratio, a difference was noticed in the iodine number of AC. When the IR was less than 2, a lower amount of H_3PO_4 participated in the formation of the carbon skeleton and pore development; therefore, the iodine number was relatively low. When the IR exceeded 2, the iodine number was reduced and reached a maximum (820.84 mg/g) when the IR was 2. However, a further increase in the ratio could make the produced micropores broaden into holes, which is closely related to the dehydration condensation effect (Li et al., 2016). AC yield ranges from 27.9% to 32.2%.

3.1.2 Microwave power

Figure 1B shows that along with the increase in microwave power, the iodine number dramatically increased, but the yield was continuously reduced. When the microwave power was 300 W, the iodine number was only 581.61 mg/g, which showed that the pores were not developed well. At a microwave power of 600 W, the iodine number reached 856.42 mg/g, indicating that higher microwave power could provide more effective carbon to generate pores (Fu et al., 2019). The decrease in yield is due to a series of deoxidation and decarboxylation reactions that occur in pyrolysis (Liang and Liu, 2020). At higher microwave power, the condensation degree of AC increases, accompanied by the production of more gas products, which ultimately leads to a decrease in yield.

3.1.3 Vacuum degree

It can be seen from Figure 1C that no indicators show a noticeable variation with the increasing vacuum degree. The iodine number of AC only increased from 787.26 mg/g to 823.39 mg/g (from -0.05 MPa to -0.06 MPa), indicating that pore structures could not be accelerated by the extension of vacuum. With the increase in vacuum degree, the yield is stable at 38%–40%.

3.1.4 Microwave irradiation time

As seen from Figure 1D, it can be seen that the iodine number of the CCAC increased significantly from 8 min to 10 min (from 824.15 mg/g to 1039.63 mg/g) because the carbon in the raw material was activated to generate more pores for release of volatile matter. The curve from 11 min to 12 min was flat, which illustrated that the easily decomposable substance reacted completely. Microwave irradiation time may cause over-carbonization, resulting in pore collapse and an increased proportion of macropores. Sufficient time must be guaranteed to ensure full carbonization and activation of the raw material (Üner and Bayrak, 2018).

3.2 Response surface analysis

3.2.1 Model result and statistical analysis

Design Expert 8.0.6 software was used to design the experiment and to statistically analyze the data. CCD with five levels and four factors was used to meet the two objectives of the current study. A complete description of each factor is given in Table 1. Table 2 shows the experimental design generated for optimization of iodine

numbers and yields for CCAC. Each experiment was carried out in triplicate and repeated twice, and the average of the experimental results was used. As shown in Table 2, the highest experimental iodine number (1039.63 mg/g) was obtained under conditions of 10 min, 500 W,-0.05 MPa, and IR 2. In contrast, total AC yield reached the highest value of 40.77% under 9 min, 600 W,-0.04 MPa, and IR 1.5. It was evident that iodine number and AC yield could not reach their maximal values simultaneously under the same preparation conditions. Among the 30 experimental runs, runs 4, 8, 12, 15, 23, and 30 had the same level of factors, and six sets of center point experiments were repeated to test the pure error of the experiment (Gonçalves and Cristiane, 2014). A small pure error indicates high experimental accuracy and high confidence in the experimental data.

The RSM-generated ANOVA analysis is shown in Tables 3, 4. The quadratic polynomial regression model was established to predict the response for iodine number and yield of CCAC. Eqn 3 and Eqn 4 can be used to predict the response for iodine number and yield, respectively. The significance of the model and that of each process variable was evaluated on the basis of their *p*-value and F-value. The significance of factors was based on the P and F values; the greater the magnitude of the F-value and correspondingly smaller the "Prob>F" value, the greater the significance of the corresponding coefficient (Goud and Das, 2021). From Table 3, it can be observed that the F-value of the model was 15.54 and the corresponding *p*-value was <0.0001, indicating the model was significant. Considering a 95% confidence interval, the factors with a *p*-value less than 0.05 were considered significant (Paramasivan and Mari, 2021). Among the process variables, IR was found to be the most significant parameter with an F-value of 57.46 and a *p*-value <0.001, followed by microwave power (an F-value of 5.74 and a *p*-value <0.05). The *p*-values of A^2, B^2, C^2, and D^2 are significant for the iodine number. As observed in Table 4, the F-value of the model was 3.82 and the corresponding *p*-value was 0.0072, indicating the model was significant. Among the process variables, IR was found to be the most significant parameter with an F-value of 24.01 and a *p*-value <0.001. The *p*-values of A^2, B^2, C^2, and D^2 were significant for yield.

R^2 is an important parameter while discussing the validity of any repression model. In this study, the R^2 values obtained were 0.935 and 0.781, indicating that 93.5% and 78.1% of the total variation were attributed to the process parameters studied, respectively. The R^2 value of 93.5% of the iodine number is greater than 90%, which indicates that the model quality is satisfactory and there is a good agreement between the experimental and predicted values. However, the R^2 of the yield (78.1%) is lower than 80%, which indicates less agreement between experimental and predicted values.

$$Y1 = 1009.52 - 78.87A + 24.93B + 13.31C + 2.64D + 1.67AB + 19.83AC + 1.23AD + 16.46BC - 8.27BD - 17.82CD - 84.69A^2 - 56.44B^2 - 67.12C^2 - 68.1D^2, \quad (3)$$

$$Y2 = 39.07 - 2.58A + 0.6B + 0.26C - 0.25D + 0.31AB + 1.3AC - 0.03AD + 0.5BC - 0.38CD - 1.38A^2 - 0.8B^2 - 1.52C^2 - 1.62D^2, \quad (4)$$

3.2.2 Respond surface analysis

The 3D curve of the response surface was plotted using Design-Expert 8.0.6 software in order to explore the interactive effect of the two factors on iodine number and yield of AC. Figures 2, 3 illustrate, respectively, the response surface analysis of IR, microwave power, microwave irradiation time, and vacuum degree on the combined effects of iodine number and yield. Each interaction contour in these figures is elliptical, demonstrating how strongly the two components in the diagram interact. The interplay between IR and power on iodine number is depicted in Figure 2A, with vacuum and microwave irradiation duration at level 0. Figure 2A shows that, in the experimental range, the iodine number first increases and then decreases as the IR increases. However, if the IR stays constant, the change in iodine number with increasing power is not statistically significant. With vacuum and power set to 0, Figure 2B illustrates the interaction impact of IR and microwave irradiation period on iodine number. As demonstrated in Figure 2B, the effect of the microwave irradiation period on the iodine number is not very obvious, but the change in IR had a sizable impact on the iodine number. Figure 2C shows the interactive effect of IR and vacuum degree on iodine number and microwave irradiation time and microwave power at level 0. It can be seen from Figure 2C that with the increase of vacuum degree, the iodine number first increases and then decreases; the iodine number is maximized at the highest point of the surface. A similar trend can be seen in Figure 3: each factor has an ideal value within the experimental range, and when one factor is fixed, the other factor can also locate the greatest yield point in the experimental range. Comparing the results, it can be seen that the curved surface of the IR is the biggest, meaning that its impact on the yield is the most noticeable.

3.2.3 RSM optimization and validation of the model

The optimum values for both responses (yield and iodine number of CCAC) were obtained using different sets of process parameters. In the study, Design-Expert 8.0.6 software was applied to perform numerical optimization for compromising between two responding factors. The optimized process slope shape is shown in Figure 4. The optimum conditions for maximum iodine number and yield of CCAC were IR 1.7, power 550.62 W, vacuum degree -0.05 MPa, and microwave time 9.26 min. RSM numerically optimized values for maximum CCAC iodine number and yield are summarized in Table 5. Under the optimal conditions, the iodine number and predicted yield were 970.91 mg/g and 39.15%, respectively.

The values predicted from the optimization test were validated by performing experiments. The results from these experiments showed that an iodine number of 933.38 mg/g and a yield of 37.57% were measured and that these measured values were in good agreement with the predicted values, with only minor differences 4.02% and 4.21% for CCAC iodine number and yield, respectively.

3.3 Infrared analysis of CC and CCAC

FT-IR analysis was used to qualitatively analyze the functional groups on the carbon's surface. A beam in the mid-infrared region (400–4000 cm^{-1}) is transmitted to the sample. When the beam

frequency matches the natural frequency of a particular chemical bond, resonance causes molecular motion (i.e., molecular stretching or bonding). This molecular motion is translated into peak intensity or transmittance at different wave numbers (cm^{-1}). Various functional groups and possible compounds in pyrolytic AC can be determined by infrared analysis. Figure 5 is the infrared spectrum.

According to the sample's infrared spectrum, the stretching vibration peak of the CC particle hydroxyl (-OH) is clearly visible at 3388 cm^{-1}, the C-H stretching vibration peak of the methylene and methyl groups is visible at 2922 cm^{-1}, and the stretching vibration peak of carbonyl C=O is visible at 1636 cm^{-1}.1371 cm^{-1} is a C-H bending vibration, whereas 1732 cm^{-1} and 1044 cm^{-1} are C-O-C pyramid ring skeleton vibrations. 1602 cm^{-1} and 1510 cm^{-1} are tiny absorption peaks next to the carbonyl vibration peak as lignin distinctive peaks. On the aromatic ring of lignin, 1250 cm^{-1} corresponds to the stretching vibrations of C=C and C-O, which demonstrates that cellulose is the sample's principal structural component, along with lignin and hemicellulose (Ji et al., 2022). The CCAC's infrared spectrum revealed that the AC was dehydrated as a result of the removal of hydroxyl from catalytic organic molecules and the dehydration of phosphoric acid. The absorption peak of the C=O structure vanished, and the hydroxyl peak was significantly diminished. The aromatic ring structure developed following pyrolysis was indicated by the bending vibration of 1582 cm^{-1}, which was C-H. The bending vibration of C-O is 1166 cm-1. When phosphoric acid produces phosphorus oxide, it combines with carbon to generate the C-O-P structure. As a result, no bands indicating the production of novel oxygen functional groups were seen on CCAC during microwave vacuum pyrolysis.

3.4 Characterization of CCAC using BET and SEM

Figures 6, 7 show the distribution of the N_2 adsorption and desorption isotherm and the pore size of CCAC. A porosimetry analysis was carried out to determine the specific surface area, pore diameter, and volume of CCAC. The BET surface area of CCAC was evaluated at 995.09 m^2/g. From the Barrett Joyner Halenda (BJH) model, the calculated pore volume was evaluated at 0.708 cm3/g.

The SEM images of CC and CCAC are shown in Figure 8. It can be seen that CCAC subjected to H_3PO_4 activation had significant effects. The size and shape of the pores present in CCAC are artificially created with different structures found in the raw material. The formation of pores is due to the release of volatiles within the CC by microwave heating (Li, 2020). In other words, a well-developed porous structure can be observed with a regular and homogeneous surface morphology.

4 Conclusion

This study has provided sustainable and environmentally friendly strategies for effective agricultural waste management and valorization approaches. Microwave pyrolysis of CC was carried out to produce CCAC. Effects of IR, microwave power, vacuum degree, and microwave irradiation time on CCAC iodine number and yield were investigated. The optimized parameters obtained were 550.62 W, 9.26 min, -0.05 Mpa, and 1.7 IR, with responses of 37.57% yield and 933.38 mg/g iodine. The model-predicted results were validated, and it was found that the experimental data varied only by 4.21% in yield and 4.02% in iodine number from the predicted values. The morphological and chemical characteristics of prepared CCAC evaluated using FT-IR, BET, and SEM exhibited the potential use of CCAC as an adsorbent. The application of low-cost CCAC as an adsorbent may lead to economic as well as environmental benefits by helping in the management of agricultural residue corn cobs.

Data availability statement

The original contributions presented in the study are included in the article/Supplementary Material; further inquiries can be directed to the corresponding author.

Author contributions

XH and XC were responsible for writing the manuscript, LJ was responsible for providing ideas, and XW was responsible for software.

Funding

The study acknowledges the support of grants from the education department of the National Natural Science Foundation of China (41907116), the Basic Research Program of Jiangsu Province (BK20191040), Changzhou Science and Technology Program (International Science and Technology Cooperation) Project (CZ20170020), and Jiangsu Graduate Practice Innovation Program (XSJCX22_77).

Conflict of interest

The authors declare that the research was conducted in the absence of any commercial or financial relationships that could be construed as a potential conflict of interest.

Publisher's note

All claims expressed in this article are solely those of the authors and do not necessarily represent those of their affiliated organizations, or those of the publisher, the editors, and the reviewers. Any product that may be evaluated in this article, or claim that may be made by its manufacturer, is not guaranteed or endorsed by the publisher.

References

Aditya, P., Zi, W. N., Hadibarata, T., Aziz, M., Yeo, J. Y. J., and Ismadji, S., (2022). Effects of pyrolysis temperature and impregnation ratio on adsorption kinetics and isotherm of methylene blue on corn cobs activated carbons. *S. Afr. J. Chem. Eng* 42, 91–97. doi:10.1016/j.sajce.2022.07.008

Arpia, A. A., Chen, W. H., Lam, S. S., Rousset, P., and Luna, M. D. G. (2021). Sustainable biofuel and bioenergy production from biomass waste residues using microwaveassisted heating: A comprehensive review. *J. Chem. Eng* 403, 126233–127131. doi:10.1016/j.cej.2020.126233

Czajkowski, Ł., Wojcieszak, D., Olek, W., and Przybył, J. (2019). Thermal properties of fractions of corn stover. *Constr. Build. Mater* 210, 709–712. doi:10.1016/j.conbuildmat.2019.03.092

Elsa, A., James, S., Brodie, G., Jacob, M. V., and Schneider, P. A. (2017). Biochar produced from biosolids using a single-mode microwave: Characterisation and its potential for phosphorus removal. *J. Environ. Mange* 196, 119–126. doi:10.1016/j.jenvman.2017.02.080

Fu, H. M., Hong, Q., and Zhang, C. (2022). Corn stove bioethanol production substantially contribute to China's carbon neutrality ambition? *Resour. Conserv. Recyc. Adv* 15, 210–220. doi:10.1016/j.rcradv.2022.200111

Fu, Y., Shen, Y., Zhang, Z., Ge, X., and Chen, M. (2019). Activated bio-chars derived from rice husk via one and two step KOH catalyzed pyrolysis for phenol adsorption. *Total Environ* 646, 1567–1577. doi:10.1016/j.scitotenv.2018.07.423

Gonçalves, R., Cristiane, M. V., da Silva, N. M., de Sousa, L. F., Bonomo, R. C. F., and de Souza, A. O., (2014). Preparation of activated carbons from cocoa shells and siriguela seeds using H3PO4 and ZnCl2 as activating agents for BSA and α-lactalbumin adsorption. *Fuel Process. Technol* 126, 476–486. doi:10.1016/j.fuproc.2014.06.001

Goud, V. V., and Das, S. (2021). RSM-optimised slow pyrolysis of rice husk for bio-oil production and its upgradation. *Energy* 225, 120161–120788. doi:10.1016/j.energy.2021.120161

Idris, S. S., Rahman, N. A., Ismail, K., Mohammed, Y. M. F., and Mohd, H. (2022). Microwave-assisted pyrolysis of oil palm biomass: Multi-optimisation of solid char yield and its calorific value using response surface methodology. *Front. Chem. Eng* 4, 119–133. doi:10.3389/fceng.2022.864589

Test methods of wooden activated carbon--Determination of iodine number. International Continence Society, Bristol, UK, 2015,

Ji, L. M., Yin, C., Sen, Y. D., Du, Y., and Wu, H. (2022). Changes in the pore structure of modified sludge-activated carbon and its effect on the adsorption characteristics of CO2 under high pressure. *Microporous Mesoporous Mater* 18, 112255–112801. doi:10.1016/j.micromeso.2022.112255

Ji, Y. C., Jihee, N., Yun, B. Y., Kim, Y. U., and Kim, S. (2022). Utilization of corn cob, an essential agricultural residue difficult to disposal: Composite board manufactured improved thermal performance using microencapsulated PCM. *Ind. Crops Prod* 183, 114931–115168. doi:10.1016/j.indcrop.2022.114931

Kai, G., Gang, L., and Wei, T. (2022). High-dimensional reliability analysis based on the improved number-theoretical method. *Appl. Math. Model* 37, 151–164. doi:10.1016/j.apm.2022.02.030

Kong, Y., Zhi, Z., and Peng, Y. (2022). Multi-objective optimization of ultrasonic algae removal technology by using response surface method and non-dominated sorting genetic algorithm-II. *Ecotoxicol. Environ. Saf* 56, 113151–113299. doi:10.1016/j.ecoenv.2021.113151

Li, H. Y., Huang, Y. F., Lin, X. H., Liu, Y. F., Lv, Y., and Liu, M. H.,(2022). Microwave-assisted depolymerization of lignin with synergic alkali catalysts and a transition metal catalyst in the aqueous system. *React. Chem. Eng* 7 (8), 1750–1761. doi:10.1039/d2re00091a

Li, Y. H., Chang, F. m., Huang, B., Song, Y. p., Zhao, H. y., and Wang, K. j. (2020). Activated carbon preparation from pyrolysis char of sewage sludge and its adsorption performance for organic compounds in sewage. *Fuel* 266, 117053–117181. doi:10.1016/j.fuel.2020.117053

Li, Y., Li, Y., Li, L., Shi, X., and Zhan, W. (2016). Preparation and analysis of activated carbon from sewage sludge and corn stalk. *Adv. Powder Technol* 27, 684–691. doi:10.1016/j.apt.2016.02.029

Liang, Q. L., Liu, Y. C., Chen, M., Ma, L., and Yang, B., (2020). Optimized preparation of activated carbon from coconut shell and municipal sludge. *Mater. Chem. Phys* 214, 122327–122494. doi:10.1016/j.matchemphys.2019.122327

Liew, R. K., Nam, W. L., Chong, M. Y., Phang, X. Y., Su, M. H., and Yek, P. N. Y., (2018). Oil palm waste: An abundant and promising feedstock for microwave pyrolysis conversion into good quality biochar with potential multi-applications. *Process Saf. Environ. Prot* 115, 57–69. doi:10.1016/j.psep.2017.10.005

Menardo, S., Airoldi, G., Cacciatore, V., and Balsari, P. (2015). Potential biogas and methane yield of maize stover fractions and evaluation of some possible stover harvest chains. *Biosyst. Eng* 129, 352–359. doi:10.1016/j.biosystemseng.2014.11.010

Mohamad, S. M. S., Azni, A. A., Wan Ab Karim Ghani, W. A., Idris, A., Ja'afar, M. F. Z., and Mohd Salleh, M. A. (2022). Production of biochar from microwave pyrolysis of empty fruit bunch in an alumina susceptor. *Energy* 240, 122710–122777. doi:10.1016/j.energy.2021.122710

Mong, G. R., Chong, C. T., Ng, J. H., Chong, W. W. F., Ong, H. C., and Tran, M. V. (2020). Multivariate optimisation study and life cycle assessment of microwave-induced pyrolysis of horse manure for waste valorisation and management. *Energy* 216, 119194–119199. doi:10.1016/j.energy.2020.119194

Nam, W. L., Phang, X. Y., Su, M. H., Liew, R. K., Ma, N. L., and Rosli, M. H. N. B., (2018). Production of bio-fertilizer from microwave vacuum pyrolysis of palm kernel shell for cultivation of Oyster mushroom (Pleurotus ostreatus). *Sci. Total. Env* 624, 9–16. doi:10.1016/j.scitotenv.2017.12.108

NBSC (National Bureau of Statistics of China) (2021). https://data.stats.gov.cn/english/ (Accessed January 8, 2021).

Paramasivan, B., and Mari, S. S. (2021). Evaluation of influential factors in microwave assisted pyrolysis of sugarcane bagasse for biochar production. *Environ. Technol. Innov* 24, 101939–101972. doi:10.1016/j.eti.2021.101939

Quillope, J. C. C., Carpio, R. B., Gatdula, K. M., Detras, M. C. M., and Doliente, S. S. (2021). Optimization of process parameters of self-purging microwave pyrolysis of corn cob for biochar production. *Heliyon* 34, 084177–e8511. doi:10.1016/j.heliyon.2021.e08417

Scarlett, A., Graham, B., and Mohan, V. J. (2022). Energy recovery from sugarcane bagasse under varying microwave-assisted pyrolysis conditions. *Bioresour. Technol. Rep* 20, 101283–111038. doi:10.1016/j.biteb.2022.101283

Selvam, S. M., and Paramasivan, B. (2022). Microwave assisted carbonization and activation of biochar for energy-environment nexus: A review. *Chem* 286, 131631–131648. doi:10.1016/j.chemosphere.2021.131631

Shin, Y. F., Syazana, A., Liew, R. K., Yek, P. N. Y., and Lam, S. S. (2020). Production of biochar for potential catalytic and energy applications via microwave vacuum pyrolysis conversion of cassava stem. *Mater. Sci. Energy Technol* 56, 728–733. doi:10.1016/j.mset.2020.08.002

Shukla, N., Sahoo, D., and Remya, N. (2019). Biochar from microwave pyrolysis of rice husk for tertiary wastewater treatment and soil nourishment. *J. Clean. Prod* 235, 1073–1079. doi:10.1016/j.jclepro.2019.07.042

Takada, M., Niu, R., Minami, E., and Saka, S. (2018). Characterization of three tissue fractions in corn (Zea mays) cob. *Biomass Bioenergy* 115, 130–135. doi:10.1016/j.biombioe.2018.04.023

Tayra, R. B., Maraísa, G., Junior, M. S., and Rezende, M. C. (2022). Sustainable process to produce activated carbon from Kraft lignin impregnated with H3PO4 using microwave pyrolysis. *Bio. Bio* 156, 106333–111130. doi:10.1016/j.biombioe.2021.106333

Tsai, W. T., Chang, C. Y., Wang, S. Y., Chang, C. F., Chien, S. F., and Sun, H. F. (2001). Cleaner production of carbon adsorbents by utilizing agricultural waste corn cob. *Resour. Conserv. Recycl* 32, 43–53. doi:10.1016/S0921-3449(00)00093-8

Üner, O., and Bayrak, Y. (2018). The effect of carbonization temperature, carbonization time and impregnation ratio on the properties of activated carbon produced from Arundo donax. *Microporous Mesoporous Mater* 268, 225–234. doi:10.1016/j.micromeso.2018.04.037

Wan, A. W. M., Wai, L. N., Sonne, C., Peng, W., Phang, X. Y., and Liew, R. K., (2020). Applying microwave vacuum pyrolysis to design moisture retention and pH neutralizing palm kernel shell biochar for mushroom production. *Bioresour. Technol* 312, 123572–124236. doi:10.1016/j.biortech.2020.123572

Wan, M. W. A., Chong, C. T., Lam, W. H., Anuar, T. N. S. T., Ma, N. L., and Ibrahim, M. D., (2018). Microwave co-pyrolysis of waste polyolefins and waste cooking oil: Influence of N2 atmosphere versus vacuum environment. *Energy Convers. manage* 171, 1292–1301. doi:10.1016/j.enconman.2018.06.073

Yang, Q., Zhou, H. W., Bartocci, P., Fantozzi, F., Masek, O., and Agblevor, F. A., (2022). Prospective contributions of biomass pyrolysis to China's 2050 carbon reduction and renewable energy goals. *Nat. Commun* 230, 1698–1745. doi:10.1038/s41467-021-21868-z

Yek, P. N. Y., Liew, R. K., Osman, M. S., Lee, C. L., Chuah, J. H., and Park, Y. K., (2019). Microwave steam activation, an innovative pyrolysis approach to convert waste palm shell into highly microporous activated carbon. *J. Environ. Mange* 236, 245–253. doi:10.1016/j.jenvman.2019.01.010

Yu, H., Qu, J., Liu, Y., Yun, H., Li, X., and Zhou, C., (2022). Co-Pyrolysis of biomass and polyvinyl chloride under microwave irradiation: Distribution of chlorine. *Sci. Total Environ* 806, 150903–151245. doi:10.1016/j.scitotenv.2021.150903

Zi, W., Chen, Y., Pan, Y., Zhang, Y., He, Y., and Wang, Q. (2019). Pyrolysis, morphology and microwave absorption properties of tobacco stem materials. *Sci. Total Environ* 683, 341–350. doi:10.1016/j.scitotenv.2019.04.053